JMEPEG (1999) 8:693-700

Wear Response of a Zn-Base Alloy in the Presence of SiC Particle Reinforcement: A Comparative Study with a Copper-Base Alloy

B.K. Prasad, S. Das, O.P. Modi, A.K. Jha, R. Dasgupta, and A.H. Yegneswaran

(Submitted 21 December 1998; in revised form 7 July 1999)

An attempt has been made in this study to examine the effects produced by the reinforcement of (10 wt%) SiC particles on the sliding wear behavior of a Zn-base alloy. The matrix alloy was also subjected to identical test conditions to assess the influence of the SiC dispersoid phase. The wear characteristics of the (Zn-base alloy) composite and the matrix alloy were also compared with those of a Cu-base alloy (i.e., an aluminum bronze) in order to understand the scope of exploiting the Zn-base alloy matrix/composite as a substitute material for the latter (Cu-base) alloy.

It has been observed that low frictional heat generated at the lower sliding speed (0.42 m/s) enabled the Zn-base (matrix) alloy to perform better than the composite material, while the Cu-base alloy showed intermediate wear resistance. On the contrary, the trend changed at a higher sliding speed (4.62 m/s) when high frictional heating caused the wear behavior of the Cu-base alloy to be superior to that of the Zn-base (matrix) alloy. The composite in this case performed better than the matrix alloy.

The wear behavior of the specimens has been explained in terms of factors like microcracking tendency and thermal stability introduced by the SiC dispersoid phase and lubricating, load bearing, and low melting characteristics of microconstituents like α and η in the (Zn-base) alloy system and the thermal stability of the Cu-base alloy. It seems that the predominance of one set of parameters over the other actually controls the overall performance of a material. Once again, it is the test conditions that ultimately allow a particular set of factors to govern the other and influence the response of the specimens accordingly. The observed wear behavior of the samples has been substantiated further with their wear surface characteristics.

Keywords sliding wear, zinc-base alloy, zinc-base alloy-SiC composite

1. Introduction

Zn-base alloys comprising 8-28% aluminum (Al), 1-3% copper (Cu), and ~0.05% magnesium (Mg) have been observed to be cost-effective and energy-effective substitutes to a variety of ferrous and nonferrous alloys (Ref 1-3). However, one of the major shortcomings of the Zn-base alloys is their inferior properties at temperatures exceeding ~100 °C (Ref 1-3). Accordingly, the variety of Zn-base alloys is suitable for use in tribological as well as general engineering applications involving operating temperatures not exceeding the limit (Ref 1-3). In a recent study, increasing the Al content of the alloy system (to ~37.5%) has been observed to attain improved mechanical and sliding wear properties at higher test temperatures and speeds respectively, although within limits (Ref 4). Further, incorporation of hard second-phase particles (SPPs) in the alloy matrix has also exhibited better elevated temperature (mechanical) properties (Ref 5-11). However, the effects of the SPP reinforcement on the sliding wear characteristics of the alloy system seem to have been studied to a limited extent (Ref 9-11). In this context, a comparison of the sliding wear performance of the matrix alloy and its composite, comprising hard dispersoid phase, could be quite interesting. Further, an assessment of the working capability of the alloy/composite with that of a conventional material could enable one to have an idea of the suitability of the developed Zn-base alloy/composite for engineering applications.

In view of the above, an attempt has been made to understand the effects produced through reinforcing a Zn-37.2% Al-base alloy with hard SiC (silicon carbide) particles on its sliding wear characteristics under varying test speeds and pressures. The matrix (Zn-base) alloy has also been processed in a manner similar to that for processing the composite and subjected to identical test conditions in order to examine the role played by the SiC dispersoid phase. Further, the behavior of the Zn-base matrix alloy/composite has also been compared with that of a Cu-base alloy (i.e., an aluminum bronze) under the test conditions in order to have some idea about the working capability of the developed (Zn-base) alloy/composite with respect to the conventionally used material (bronze).

B.K. Prasad, S. Das, O.P. Modi, A.K. Jha, R. Dasgupta, and **A.H. Yegneswaran,** Regional Research Laboratory (CSIR), Bhopal-462 026, India.

2. Experimental

2.1 Material Preparation

The experimental alloys and composite (Table 1) were prepared by the liquid metallurgy route in the form of 20 mm diameter, 150 mm long cylindrical castings using cast iron molds. For preparing the composite, 10 wt% SiC particles (size 50-100 μm) were dispersed in the alloy melt with the help of a mechanical stirrer.

2.2 Microstructural Studies and Measurement of Hardness and Density

Metallographically prepared specimens were used for microstructural characterization. The sample of the Cu-base alloy was etched with potassium dichromate solution, whereas the samples of the Zn-base alloy/composite were etched with diluted aqua regia. Hardness and density of the metallographically prepared samples were also measured as per the procedures discussed elsewhere (Ref 12, 13).

2.3 Sliding Wear Tests

Dry sliding wear tests were conducted on 8 mm diameter, 53 mm long cylindrical pins against an EN25 (Fe-0.3%C-0.7%Cr-2.5%Ni-0.5%Mo) steel disc having HRC 32. The equipment used for carrying out the wear tests was a Cameron-Plint (United Kingdom) pin-on-disc machine (Fig. 1). Test speeds adopted for the samples were 0.42 and 4.62 m/s, whereas pressure on the specimens was increased in steps until specimen seizure was indicated (as evidenced by a sudden rise in wear rate, large adhesion/fusion of the pin material onto the disc, and abnormal noise from the pin-disc assembly), prior to traversing a fixed sliding distance of 500 m. Wear rate was computed by weight loss technique using a Mettler-Toledo, Inc. (Columbus, OH) microbalance. The specimens were cleaned thoroughly prior to and after the wear tests. Temperature rise (near the specimen surface) was monitored as a function of test duration by inserting a chromel-alumel thermocouple in a hole made at a distance of 1.5 mm from the contacting surface of the samples. The temperature so recorded, though, does not represent a true measure of the actual temperature at the contacting surfaces of the specimens, yet it can be considered to at least qualitatively represent the relative (frictional heating) behavior of the samples being studied.

2.4 Examination of Wear Surfaces

Wear surfaces of typical samples were examined using scanning electron microscopy (SEM). The specimens were mounted on brass studs and sputtered with gold prior to their SEM examination.

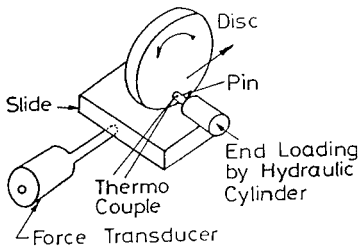

Fig. 1 A schematic representation of the pin-on-disc machine

3. Results

3.1 Microstructure

Figure 2 shows the microstructural characteristics of the experimental alloys. The (Zn-base alloy) composite revealed a reasonably uniform distribution of the dispersed SiC particles in the matrix (Fig. 2a) and good dispersoid/matrix bonding (Fig. 2b). Different microconstituents of the (Zn-base) matrix alloy such as primary α dendrites, eutectoid $\alpha + \eta$ and ε phase (Fig. 2c, regions marked by A, B, and by single arrow, respectively) have been characterized and discussed elsewhere (Ref 12-14). Important microstructural phases in the case of the Cu-base alloy included the primary α dendrites, Cu-Al intermetallic compound along with fine particles of iron (Fig. 2d, regions marked by A, C, and the double arrow, respectively) as discussed elsewhere (Ref 15).

3.2 Hardness and Density

Table 1 represents various properties of the specimens. The composite attained somewhat higher hardness than the corresponding (Zn-base) matrix alloy while that of the Cu-base alloy was the maximum. So far as the density of the specimens is concerned, it was highest for the Cu-base alloy followed by that of the Zn-base matrix alloy and the composite.

3.3 Sliding Wear Characteristics

Figure 3 represents the wear rate of the samples as a function of applied pressure. The influence of sliding speed can also be noted in the figure. Wear rate was observed to increase with pressure at all the test speeds. However, the rate of increase in the wear rate was low, up to a specific pressure, which was followed by a higher rate of enhancement in wear rate at higher pressures. This was the trend observed over the entire range of test conditions except in the case of Zn-base matrix alloy and the Cu-base alloy at 4.62 m/s (Fig. 3). In the latter case, the wear rate increased with pressure practically at a constant rate. Further, the Zn-base (matrix) alloy attained minimum wear loss at 0.42 m/s while the (Zn-base alloy) composite exhibited the maximum wear loss. The copper-base alloy showed an intermediate response. The trend changed slightly at 4.62 m/s in the sense that the Cu-base alloy delineated the least wear rate followed by that of the (Zn-base alloy) composite and that of the Zn-base (matrix) alloy (Fig. 3).

Table 1 Chemical composition and properties of the specimens

Specimen No.	Type	Composition, wt%					Vickers hardness	Density, g/cm^3
		Zn	Al	Cu	Mg	Fe		
1	Zn-base matrix alloy	bal	37.5	2.5	0.2	…	125	4.45
2	Zn-base alloy composite (a)	…	…	…	…	…	135	4.41
3	Cu-base alloy	…	10.3	bal	…	1.5	159	7.55

(a) Specimen No. 2 is a matrix alloy per specimen No. 1, dispersed with 10 wt% SiC particles.

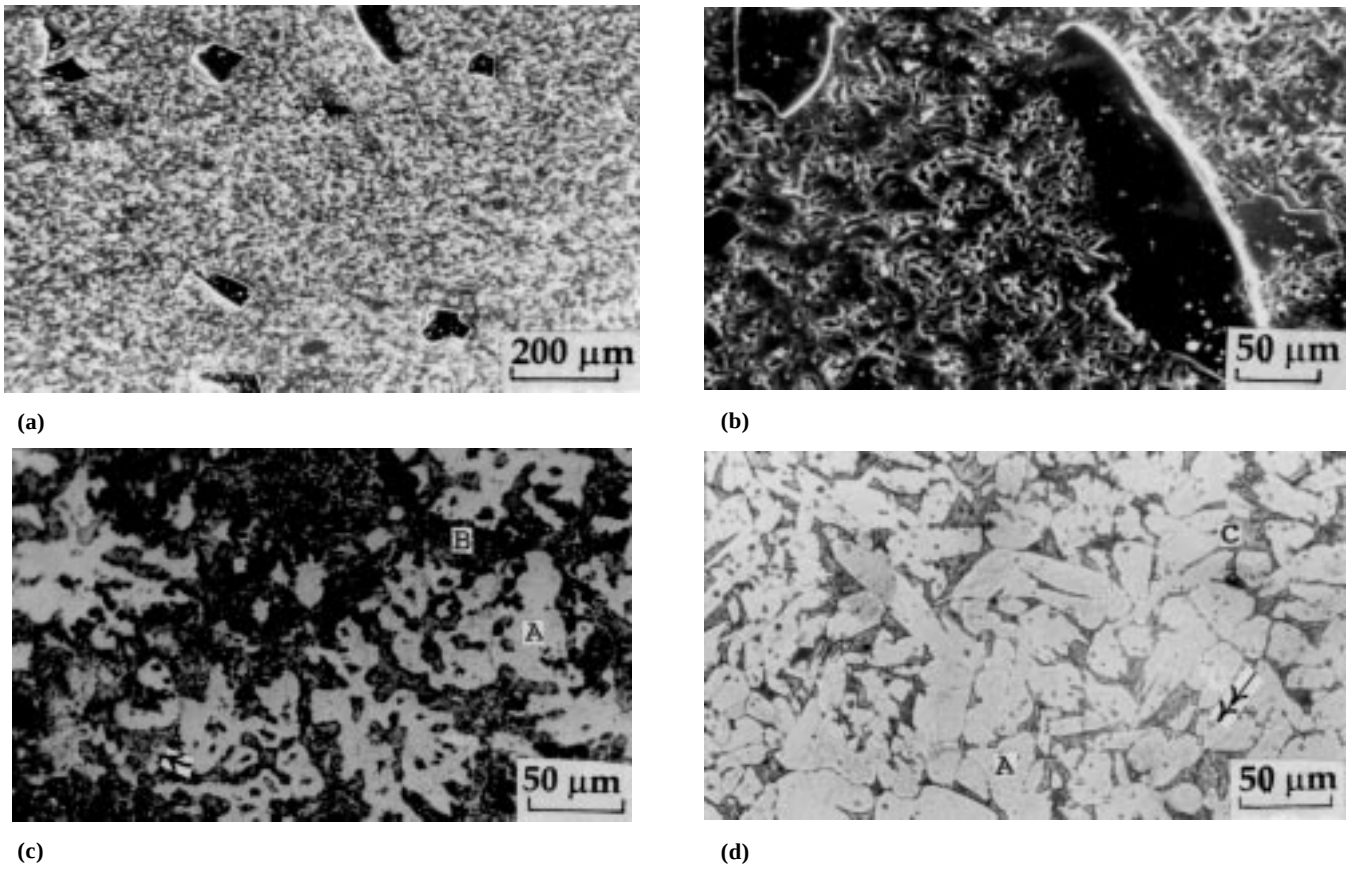

Fig. 2 Microstructure of (a and b) the Zn-base alloy composite, (c) the Zn-base matrix alloy, and (d) the Cu-base alloy. A, primary α; B, eutectoid α and η; single arrow, ε; C, Cu-Al intermetallic compound; double arrow, iron particle

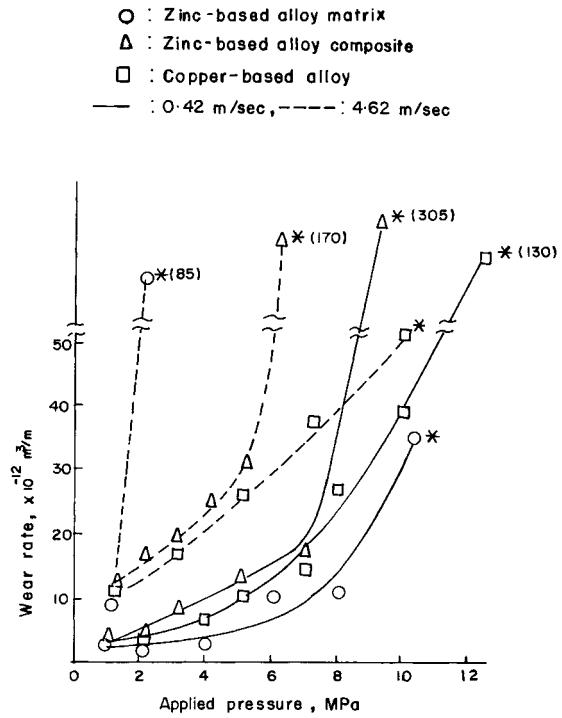

Fig. 3 Wear rate versus applied pressure plots at different sliding speeds

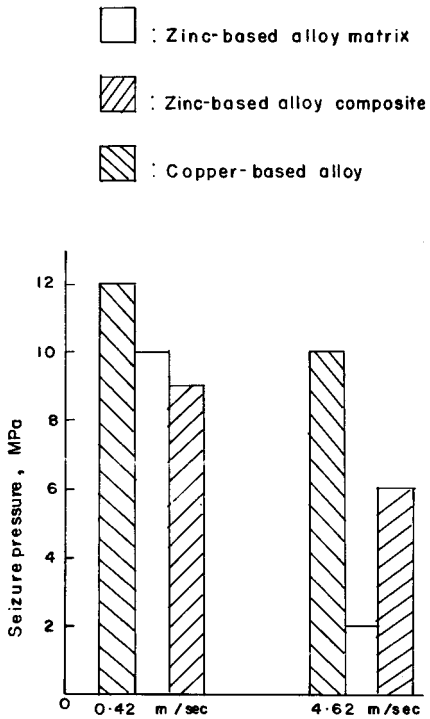

Fig. 4 Seizure pressure of the specimens at different sliding speeds

Seizure pressures of the samples at different sliding speeds are shown in Fig. 4. At 0.42 m/s of sliding, maximum seizure resistance (pressure) was observed in the case of the Cu-base alloy. The Zn-base (matrix) alloy seized at a pressure higher than that at which the (Zn-base alloy) composite seized. However, at the sliding speed of 4.62 m/s, the seizure behavior of the (Zn-base alloy) composite was observed to be better than that of the Zn-base (matrix) alloy; the Cu-base alloy once again revealed highest seizure pressure (Fig. 4).

Temperature near the sliding surface of the samples has been plotted as a function of test duration at different speeds in Fig. 5. The extent of frictional heating increased with test duration, wherein the rate of heating was higher in the beginning of the tests, preceding a reduced rate of heating at longer test duration at both the sliding speeds. Further, the specimens attained larger frictional heating as the sliding speed/pressure increased. At 0.42 m/s, the Zn-base (matrix) alloy experienced least frictional heating while the Cu-base alloy suffered from maximum degree of heating, and the (Zn-base alloy) composite revealed intermediate behavior (Fig. 5a). In the event of sliding at 4.62 m/s, all the varieties of samples showed the attainment of a comparable level of heating at the minimum applied pressure (Fig. 5b). The trend changed at a higher test pressure at the speed wherein minimum frictional heating occurred in the case of the Zn-base (matrix) alloy prior to its seizure; seizure caused higher frictional heating (Fig. 5b). The (Zn-base alloy) composite experienced an intermediate level of frictional heating, while the level was the maximum for the Cu-base alloy (Fig. 5b).

Maximum temperature near the sliding surface of the specimens has been plotted as a function of applied pressure at different speeds (Fig. 6). The extent of frictional heating increased with pressure and speed. Moreover, least frictional heating was noted for the Zn-base (matrix) alloy at 0.42 m/s, whereas that for the Cu-base alloy was the maximum. The (Zn-base alloy) composite attained an intermediate level of heating (Fig. 6). On the contrary, at 4.62 m/s, the Zn-base (matrix) alloy attained higher frictional heating than did the (Zn-base alloy) composite.

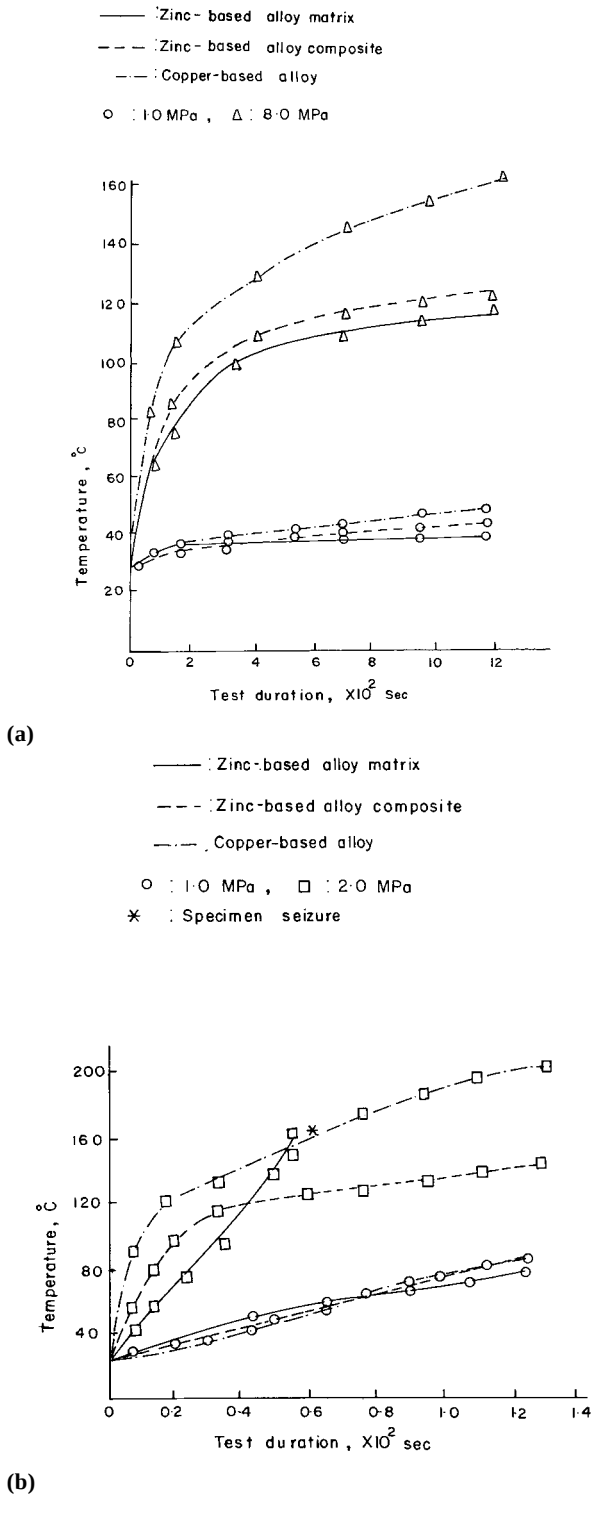

Fig. 5 Temperature near the specimen surface versus test duration plots at (a) 0.42 and (b) 4.62 m/s

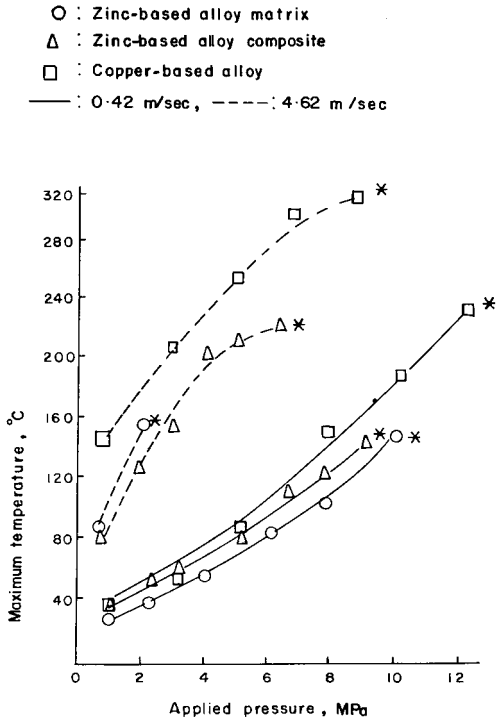

Fig. 6 Maximum temperature near the specimen surface plotted as a function of applied pressure at different speeds

However, the Cu-base alloy experienced maximum frictional heating in this case also (Fig. 6).

3.4 Wear Surfaces

Wear surfaces of the composite are shown in Fig. 7. Limited surface damage was observed when the tests were conducted at low pressures at the sliding speed of 0.42 m/s (Fig. 7a). Increasing the pressure at the speed led to the generation of more severely damaged wear surfaces (Fig. 7b). Arrow-marked regions in Fig. 7(b) are typical examples of microcracking on the wear surfaces. The extent of (wear) surface damage decreased somewhat at low pressures when the sliding speed was raised to 4.62 m/s (Fig. 7c). Sticking of debris particles on the wear surface was also noted (Fig. 7c, regions marked A). A magnified view clearly shows the sticking debris (Fig. 7d). The extent of damage to the specimen surface increased with pressure at the (higher) speed (Fig. 7c versus 7e). Furthermore, the extent of microcracking of the samples decreased with increasing speed (Fig. 7e versus 7b).

The wear surfaces of the Zn-base (matrix) alloy were smooth at low pressures at the speed of 0.42 m/s (Fig. 8a). Sticking of debris particles was also observed in this case (Fig. 8a, region marked by arrow). Higher pressures at the speed considerably increased the severity of surface damage (Fig. 8b). Similar was the trend observed at 4.62 m/s with greater surface damage (Fig. 8c and d) than at the lower speed (Fig. 8a and b).

(a)

(b)

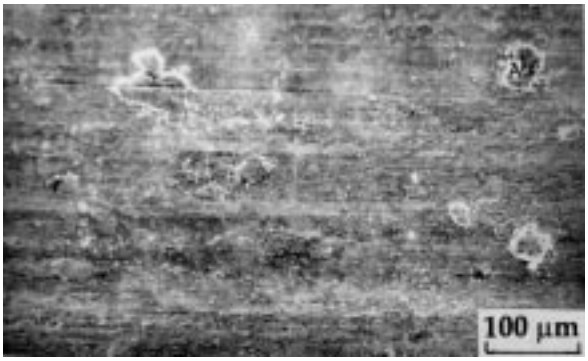

(c)

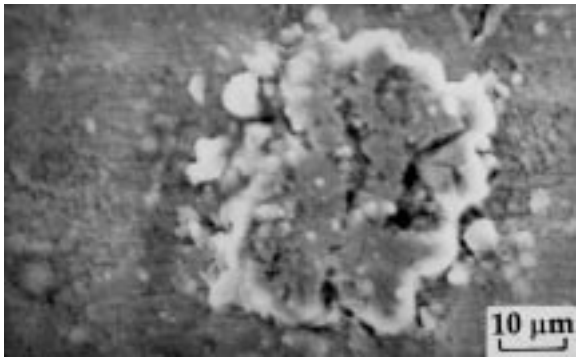

(d)

(e)

Fig. 7 Wear surfaces of the Zn-base alloy composite. (a) Tested at 0.42 m/s at the applied pressure of 1.0 MPa. (b) Tested at 0.42 m/s at the applied pressure of 9.0 MPa. (c) Tested at 4.62 m/s at the applied pressure of 1.0 MPa. (d) Tested at 4.62 m/s at the applied pressure of 1.0 MPa. (e) Tested at 4.62 m/s at the applied pressure of 6.0 MPa. Arrow, microcracking; A, sticking of debris

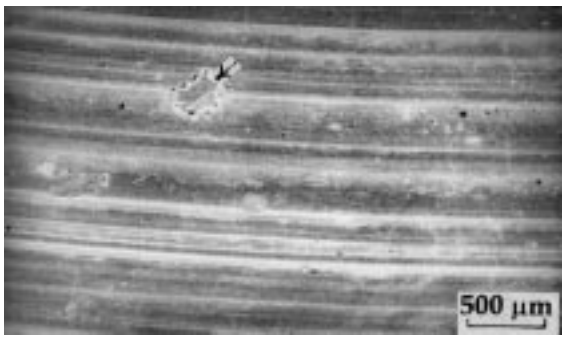

(a)

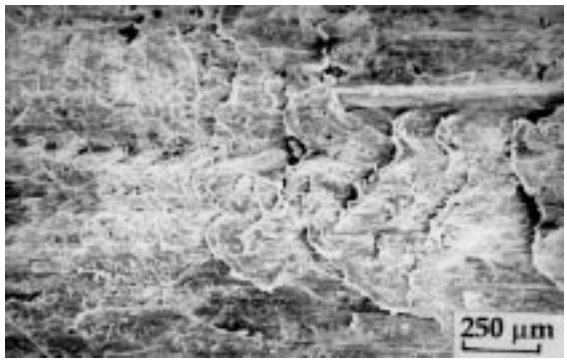

(b)

(c)

(d)

Fig. 8 Wear surfaces of the Zn-base matrix alloy. (a) Tested at 0.42 m/s at the applied pressure of 1.0 MPa. (b) Tested at 0.42 m/s at the applied pressure of 10.0 MPa. (c) Tested at 4.62 m/s at the applied pressure of 1.0 MPa. (d) Tested at 4.62 m/s at the applied pressure of 2.0 MPa. Arrow, sticking of debris

The Cu-base alloy tested at low pressures at the sliding speed of 0.42 m/s revealed partially damaged wear surfaces (Fig. 9a) whose extent and severity increased considerably with rising pressure (Fig. 9b versus 9a) and speed (Fig. 9c versus 9a).

4. Discussion

Wear behavior of the specimens exhibited under different test conditions can be explained in terms of specific features of their various microconstituents. For example, the α and η (the

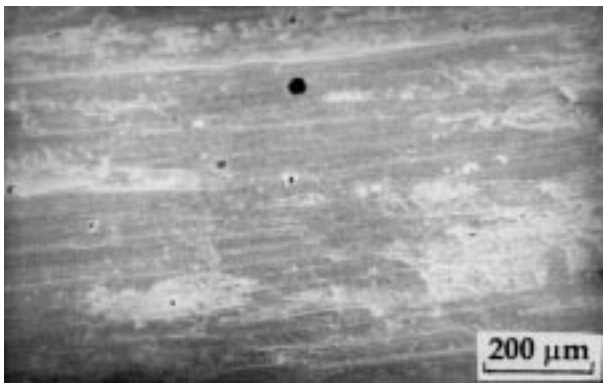

(a)

(b)

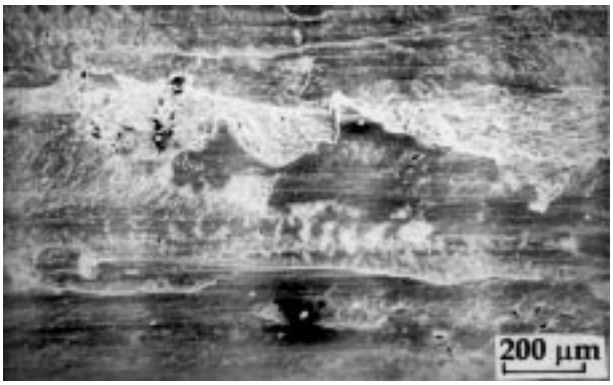

(c)

Fig. 9 Wear surfaces of the Cu-base alloy. (a) Tested at 0.42 m/s at the applied pressure of 1.0 MPa. (b) Tested at 0.42 m/s at the applied pressure of 12.0 MPa. (c) Tested at 4.62 m/s at the applied pressure of 1.0 MPa

major constituents) in the Zn-base matrix alloy (Fig. 1c) are soft and have low melting characteristics. Accordingly, they impart load bearing and solid lubrication characteristics (Ref 16, 17), which become effective under test conditions involving low frictional heating because of their inferior thermal stability (Ref 15, 18). On the contrary, test conditions (Ref 15, 16) causing the generation of higher frictional heat make the (Zn-base matrix) alloy prone to adhere to the disc surface to a considerable extent. As a result, the (α and η) constituent phases fail to produce their positive effects (Ref 15, 19). Generation of excessively high frictional heat leads to mass fusion of the specimen material onto the disc surface resulting in specimen seizure (Ref 20). Addition of hard second phase particles (SPPs) like SiC to a metallic matrix introduces a microcracking tendency in the matrix, where the dispersoid/matrix interfacial regions act as potential sites for the nucleation and propagation of microcracks (Ref 18, 20-22). The dispersoid phase also imparts thermal stability to the alloy system allowing a more effective load transfer between the matrix and the (dispersoid) phase (Ref 7). This creates a situation favorable for more effective working of the softer and low melting (α and η) microconstituents, while the microconstituents provide support to the dispersoid particles (Ref 19). Microcracking tendency predominates at lower operating temperatures and deteriorates the wear performance of materials, while the opposite is true for thermal stability (Ref 18, 19).

As for the nature of the Cu-base alloy, it does not comprise any crack-sensitive microconstituent (like the dispersoid SiC in the composite), nor does it contain any lubricating phase (such as η in the Zn-base matrix alloy). However, the Cu-base alloy possesses excellent thermal stability (Ref 15).

Based on the discussed characteristics of different microconstituents, the wear response of the specimens can now be explained. At a low sliding speed (i.e., 0.42 m/s) involving the generation of low frictional heat (Fig. 5 and 6), the Zn-base (matrix) alloy exhibited minimum wear loss (Fig. 3) as its microconstituents could perform their positive roles of load bearing and solid lubrication quite effectively due to low operating temperatures. Under the circumstances, the (Zn-base alloy) composite experienced maximum wear loss due to the predominating effect of microcracking tendency (Fig. 7b) resulting from the presence of the dispersoid SiC particles therein (Fig. 3). This also caused the composite to attain seizure resistance inferior to that of the Zn-base (matrix) alloy (Fig. 3 and 4). The absence of a lubricating microconstituent in the Cu-base alloy (like η in the Zn-base matrix alloy) led to its wear behavior being inferior to that of the Zn-base (matrix) alloy. At the same time, however, the Cu-base alloy performed better than the composite, as the former did not contain any crack-sensitive phase (like SiC in the composite). High thermal stability of the Cu-base alloy also enabled it to exhibit maximum seizure resistance (Fig. 3 and 4). Better wear response of the specimens also agreed with the generation of smoother and less damaged wear surfaces (Fig. 7-9).

During testing at 4.62 m/s, frictional heat generated was much higher than that generated at 0.42 m/s (Fig. 5 and 6). This led to the most inferior wear response of the Zn-base matrix alloy (Fig. 3 and 4) wherein the (soft and low melting) α and η phases failed to play their positive roles and, rather, their tendency towards large adhesion/fusion with the disc surface increased greatly. This was further substantiated through more severe damage of the wear surfaces (Fig. 8c and d). The thermal stability imparted by the SiC dispersoid phase however improved the wear characteristics of the composite considerably over those of the Zn-base matrix alloy (Fig. 3-6), as also evidenced by the reduced extent of damage to the wear surfaces in the latter case (Fig. 7c and d versus 8c and d). Once again, the high thermal stability of the Cu-base alloy (Ref 15) led to its best wear resistance among all types of specimens (Fig. 3 and 4), which also corroborated with its relatively improved wear surface characteristics (Fig. 9c and 8c).

The higher rate of frictional heating in the beginning of the wear tests (Fig. 5) could be attributed to the abrasion caused by the broken asperities that get entrapped between the mating surfaces in subsequent passes (Ref 20). As sliding progresses further, the effective area of contact increases in view of the changing mode of contact from asperity-to-asperity to area-to-area. This leads to a reduced level of stressing on the contacting regions and, hence, to a decreased rate of frictional heating at longer test duration (Fig. 5).

Sticking of the debris particles on to the wear surfaces (Fig. 7c and d and 8a) results from their entrapment in between the contacting surfaces in subsequent passes after their formation. The stuck debris protects the mating surfaces by reducing the extent of direct contact between the two, thereby improving the wear response of the samples (Fig. 3-6). Stick-slip/torn-off appearance on the wear surfaces (Fig. 8b-d) results from large adhesion through fusion of the specimen material with the counterface under the conditions of severe wear.

5. Conclusions

A critical appraisal of the observations made in this study clearly suggests that with material characteristics remaining unchanged, the test conditions make significant contribution toward controlling the wear characteristics of the alloys/composite. For example, low operating temperatures generated at low speed (0.42 m/s) enabled the Zn-base (matrix) alloy to perform better than the more crack sensitive (Zn-base alloy) composite material, while the Cu-base alloy performed intermediately well between the two. Seizure resistance was maximum for the (Cu-base) alloy. On the contrary, the trend changed at a higher sliding speed wherein high frictional heating led to better wear performance of the Cu-base alloy followed by that of the (Zn-base alloy) composite and the Zn-base (matrix) alloy. Thus, crack sensitivity and thermal stability appear to be the most important parameters, which become predominant over each other depending on the conditions of testing to govern the wear performance of the alloys/composite accordingly.

References

1. E.J. Kubel, Jr., Expanding Horizons for ZA Alloys, *Adv. Mater. Process.*, Vol 132, 1987, p 51-57
2. T.S. Calayag, Zinc Alloys Replace Bronze in Mining Equipment Bushings and Bearings, *Min. Eng.*, Vol 35, 1983, p 727-728
3. D. Apelian, M. Paliwal, and D.C. Herrschaft, Casting with Zinc Alloys, *J. Met.*, Vol 33, 1981, p 12-19

4. B.K. Prasad, A.K. Patwardhan, and A.H. Yegneswaran, Effects of Aluminum Content on the Physical, Mechanical and Sliding Wear Properties of Zn-base Alloys, *Z. Metallkd.*, Vol 88, 1997, p 333-338
5. M.A. Dellis, J.P. Keustermans, and F. Delannay, Zn-Al Alloy Matrix Composites: Investigations of the Thermal Expansion, Creep Resistance and Fracture Toughness, *Mater. Sci. Eng.*, Vol 135A, 1991, p 253-257
6. A.A. Das, A.J. Clegg, B. Zantout, and M.M. Yakoub, Solidification under Pressure: Aluminum and Zinc Alloys Containing Discontinuous Fibers, *Proc. Cast Reinforced Metal Composites*, S.G. Fishman and A.K. Dhingra, Ed., ASM International, 1988, p 139-147
7. L.D. Bailey, S. Dionne, and S.H. Lo, The Fracture Behavior of Squeeze Cast Zn-Al Composites, *Proc. Fundamental Relationship between Microstructure and Properties of Metal Matrix Composites*, P.K. Liaw and M.N. Gungor, Ed., The Minerals, Metals and Materials Society, 1990, p 23-25
8. S. Muthukumaraswamy and S. Seshan, *Structure and Properties of Fiber Reinforced Zn-27% Al Alloy Based MMCs*, *Composites*, Vol 26, 1995, p 387-393
9. S.H.J. Lo, S. Dionne, M. Sahoo, and H.M. Hawthorne, Mechanical and Tribological Properties of Zinc-Aluminum Metal Matrix Composites, *J. Mater. Sci.*, Vol 27, 1992, p 5681-5691
10. H.X. Zhu and S.K. Liu, Mechanical Properties of Squeeze Cast Zinc Alloy Matrix Composites Containing α-Alumina Fibers, *Composites*, Vol 5, 1993, p 437-442
11. N.B. Dahotre, T.D. McCay, and M.H. McCay, Laser Surface Modification of Zinc-Base Composites, *J. Met.*, Vol 42, 1990, p 44-47
12. B.K. Prasad, A.K. Patwardhan, and A.H. Yegneswaran, Microstructure-Property Characterization of Some Zn-Base Alloys: Effects of Heat Treatment Parameters, *Z. Metallkd.*, Vol 87, 1996, p 967-972
13. B.K. Prasad, A.K. Patwardhan, and A.H. Yegneswaran, Influence of Heat Treatment Parameters on the Microstructure and Properties of Some Zinc-Base Alloys, *J. Mater. Sci.*, Vol 31, 1996, p 6317-6324
14. B.K. Prasad, Influence of Heat Treatment on the Physical, Mechanical and Tribological Properties of a Zn-base Alloy, *Z. Metallkd.*, Vol 87, 1996, p 226-232
15. B.K. Prasad, Dry Sliding Wear Response of Some Bearing Alloys as Influenced by the Nature of Microconstituents and Sliding Conditions, *Metall. Mater. Trans.*, Vol 28A, 1997, p 809-815
16. S. Murphy and T. Savaskan, Comparative Wear Behavior of Zn-Al Based Alloys in an Automotive Engine Application, *Wear*, Vol 98, 1984, p 151-161
17. S.W.K. Morgan, Ed., *Zinc and Its Alloys and Compounds*, 1st ed., Ellis Horwood Limited Publishers, Chicestor, 1985, p 154-164
18. B.K. Prasad, A.K. Patwardhan, and A.H. Yegneswaran, Dry Sliding Wear Characteristics of Some Zinc-Aluminum Alloys: A Comparative Study with a Bearing Bronze at a Slow Speed, *Wear*, Vol 199, 1996, p 142-151
19. B.K. Prasad, A.K. Patwardhan, and A.H. Yegneswaran, Characterization of the Wear Response of a Modified Zn-Based Alloy vis-a-vis a Conventional Zn-based Alloy and Bearing Bronze at a High Sliding Speed, *Metall. Mater. Trans.*, Vol 27A, 1996, p 3513-3523
20. O.P. Modi, B.K. Prasad, A.H. Yegneswaran, and M.L. Vaidya, Dry Sliding Wear Behavior of Squeeze Cast Aluminum Alloy-Silicon Carbide Composites, *Mater. Sci. Eng.*, Vol 151A, 1992, p 235-245
21. B.S. Mazumdar, A.H. Yegneswaran, and P.K. Rohatgi, Strength and Fracture Behavior of Metal Matrix Particulate Composites, *Mater. Sci. Eng.*, Vol 68, 1984, p 85-96
22. B.K. Prasad and S. Das, The Significance of the Matrix Microstructure on the Solid Lubrication Characteristics of Graphite in Aluminum Alloys, *Mater. Sci. Eng.*, Vol 144A, 1991, p 229-235